

Published in final edited form as:

Mol Cell. 2012 July 13; 47(1): 111–121. doi:10.1016/j.molcel.2012.04.020.

NEMO ensures signaling specificity of the pleiotropic IKK β by directing its kinase activity towards I κ B α

Bärbel Schröfelbauer^{1,2}, Smarajit Polley², Marcelo Behar^{1,2}, Gourisankar Ghosh², and Alexander Hoffmann^{1,2}

¹Signaling Systems Laboratory, University of California, San Diego, 9500 Gilman Dr, La Jolla, CA 92093-0375

²Department of Chemistry and Biochemistry, University of California, San Diego, 9500 Gilman Dr, La Jolla, CA 92093-0375

Summary

Besides activating NF κ B by phosphorylating I κ Bs, IKK α /IKK β kinases are also involved in regulating metabolic insulin signaling, the mTOR pathway, Wnt signaling, and autophagy. How IKK β enzymatic activity is targeted to stimulus-specific substrates has remained unclear. We show here that NEMO, known to be essential for IKK β activation by inflammatory stimuli, is also a specificity factor that directs IKK β activity towards I κ B α . Physical interaction and functional competition studies with mutant NEMO and I κ B proteins indicate that NEMO functions as a scaffold to recruit I κ B α to IKK β . Interestingly, expression of NEMO mutants that allow for IKK β activation by the cytokine IL-1 but fail to recruit I κ Bs, results in hyperphosphorylation of alternative IKK β substrates. Furthermore IKK's function in autophagy, which is independent of NF κ B is significantly enhanced without NEMO as I κ B scaffold. Our work establishes a role for scaffolds such as NEMO in determining stimulus-specific signal transduction via the pleiotropic signaling hub IKK.

Introduction

Reliable cellular signal transduction depends on the specificity of kinases. Unlike some metabolic enzymes, in which the catalytic site may show great specificity for particular small molecule substrates, protein kinases require specificity domains. When such specificity domains are encoded by distinct specificity factors the kinase activity can in principle be directed to alternate specific substrates, allowing for functional pleiotropy (Bhattacharyya et al., 2006; Ubersax and Ferrell, 2007). One may distinguish between catalytic (or “allosteric”) specificity factors that alter the intrinsic catalytic activity of the kinase towards a specific substrate, and scaffold (or “tethering”) specificity factors that enhance otherwise weak interactions between substrate and kinase (Burack and Shaw, 2000). Whereas the c-Jun N-terminal kinase (JNK) interacting protein (JIP1), the JNK/SAPK activating protein 1 (JSAP1) and the kinase suppressor of Ras (KSR) are thought to be in the former category, the axin scaffolding proteins target the pleiotropic kinases GSK3 and CK1 to the β -catenin pathway (Burack and Shaw, 2000; Wu and Pan) (Amit et al.,

© 2012 Elsevier Inc. All rights reserved.

Correspondence to Alexander Hoffmann: ahoffmann@ucsd.edu, Tel. 858 822 4670, Fax 858 822 4671.

Publisher's Disclaimer: This is a PDF file of an unedited manuscript that has been accepted for publication. As a service to our customers we are providing this early version of the manuscript. The manuscript will undergo copyediting, typesetting, and review of the resulting proof before it is published in its final citable form. Please note that during the production process errors may be discovered which could affect the content, and all legal disclaimers that apply to the journal pertain.

2002) and the Ste5 scaffold directs the specificity of yeast MAPK signaling (Schwartz and Madhani, 2004; van Drogen and Peter, 2002). Indeed, shuffling of binding pockets of Ste5 by site-directed mutagenesis enables re-direction of signaling specificity (Dueber et al., 2003). Thus, multivalent scaffold proteins may not only direct kinase substrate specificity but also ensure signaling specificity of a pleiotropic kinase by coordinating upstream and downstream signaling axes.

The I κ B kinase (IKK) complex is ubiquitously expressed and functionally pleiotropic (Hayden and Ghosh, 2008; Scheidereit, 2006). Its major catalytic component, IKK β (also known as IKK2), was purified as the I κ B kinase that controls nuclear translocation of NF κ B to initiate pro-inflammatory gene transcription by phosphorylating the canonical I κ Bs, I κ B α , I κ B β , and I κ B ϵ (Hayden and Ghosh, 2008; Hoffmann and Baltimore, 2006; Scheidereit, 2006). However, recent literature suggests that IKK β also plays critical roles in many other biological processes including autophagy, insulin signaling and DNA damage responses, by targeting diverse alternative cellular substrates for phosphorylation (Fig. 1A) (reviewed in (Chariot, 2009; Scheidereit, 2006)).

The large number of substrates, and the diverse biological functions regulated by their phosphorylation raise the question of whether IKK β enzymatic activity may be targeted to distinct substrates. To ensure fidelity as a signal transducer of diverse signals, one would expect the activation of the kinase by upstream pathways to be coordinated with downstream substrate selection.

Results

Constitutively active IKK β requires NEMO for NF κ B activation

In response to the inflammatory cytokine IL-1 IKK β rapidly phosphorylates S32/36 of I κ B α , thereby triggering its ubiquitin-dependent proteasomal degradation, while phosphorylation of the NF κ B subunit p65 occurs with delayed kinetics (Fig. 1B, S1A). However, using purified, constitutively active IKK β (HA-IKK β EE) in an *in vitro* kinase assay, we find high phosphorylation of both I κ B α and p65 proteins with no preference for I κ B α (Fig. 1C) suggesting that *in vivo* IKK β 's preference for I κ B phosphorylation is regulated by additional factors. *In vivo*, IKK β activation in response to inflammatory cytokine and pathogen-associated molecular patterns (PAMPs) stimulation requires NEMO, which connects the kinase complex to ubiquitin chains emanating from receptor-associated signaling complexes (Israel, 2010). To test whether NEMO may also be determining the target specificity of the catalytic enzyme, we used a constitutively active form of IKK β generated through mutation of the critical activation loop serines 177 and 181 to phosphomimetic glutamates (IKK β EE). Retroviral transduction of wild-type fibroblasts with IKK β EE resulted in the expected increase in steady-state NF κ B activity, but similar expression of IKK β EE in NEMO-deficient cells had only a modest effect (Fig. 1D). However, reconstitution with retrovirally expressed NEMO restored the strong NF κ B DNA binding activity. Strikingly, *in vitro* kinase assays with immunoprecipitated IKK using either FL-I κ B α (Fig. 1D) or GST-I κ B α ₁₋₅₄ (Fig. S1B) as substrate showed that NEMO did not alter the catalytic IKK activity in these cells, suggesting that it has a specific role in the NF κ B activation pathway at a step downstream of its known function in IKK activation. Indeed, we found that IKK β EE caused only weak I κ B α phosphorylation and degradation in unstimulated NEMO-deficient cells, unless NEMO was reconstituted (Fig. 1E). Taken together these data indicate that intrinsic substrate specificity of IKK β is not sufficient for efficient I κ B phosphorylation, but that NEMO plays a role in targeting IKK activity towards the I κ B-NF κ B signaling module.

The ZF of NEMO is required for efficient phosphorylation of I κ B α

NEMO's N-terminal region interacts with IKK β , and the central CoZi-region allows for dimerization and binding to linear and K63 polyubiquitin chains, connecting IKK to inflammatory receptor pathways (Fig. 2A) (Israel, 2010). A frameshift mutation that completely removes NEMO's C-terminal Zinc finger (ZF) causes incontinentia pigmenti, its molecular function however remains unclear (Makris et al., 2002). While it is critical for NF κ B activation triggered by genotoxic stress (Huang et al., 2002), its role in inflammation-induced NF κ B activation is cell- and stimulus-specific. Disruption of the ZF was found to prevent TNF- but not IL-1 β -induced NF κ B activation in MEFs (Makris et al., 2002). A complete defect in cytokine-induced NF κ B activation was observed in human T cells expressing human C417R NEMO (corresponding to C410R in mouse NEMO) (Yang et al., 2004), while NF κ B activation by LPS was normal in mouse B-cells expressing this mutant (Huang et al., 2002). More recently the ZF has been implicated to enhance the affinity of NEMO for binding to K63 linked poly-ubiquitin chains, important for IKK activation by specific stimuli (Laplantine et al., 2009). We examined the possible role of the NEMO ZF on NF κ B activation in the context of constitutively active IKK β . We generated a truncation (Δ C25), a debilitating (C389/393S) and neutral (M408S) mutant of the ZF domain. Reconstitution of NEMO-deficient cells with these constructs resulted in expression levels comparable to those in wild-type MEFs (Fig. S2A). In cells expressing either WT or the M408S NEMO, which does not affect the overall structure of the ZF, strong NF κ B activity was detected (Fig. 2B), while only modest nuclear NF κ B activity was observed in NEMO-deficient cells. Strikingly, truncating and debilitating the ZF abolished NEMO's ability to reduce I κ B α levels (as well as I κ B β and I κ B ϵ , Fig. S2B) and to enhance NF κ B activity in the presence of IKK β EE (Fig. 2B). These data suggest that the ZF of NEMO is critical for the active IKK complex to efficiently target I κ Bs for degradation *in vivo*, to allow for NF κ B activation, even though ZF mutations had no effect on *in vitro* IKK kinase activity (Fig. S2C).

To examine NEMO's role in targeting IKK towards I κ Bs during inflammatory signaling we had to identify conditions in which NEMO mutants, defective in I κ B targeting, allowed for efficient IKK activation. NEMO-deficient cells reconstituted with NEMO mutants were exposed to TNF, IL-1 β and LPS. In cells expressing WT NEMO and M408S mutant NEMO all stimuli induced *in vitro* kinase activity, although kinase activity induced by TNF was attenuated in M408S NEMO expressing cells (Fig. 2C, S2D, S2E). IL-1 β and LPS also induced strong, yet somewhat weaker kinase activity in cells expressing NEMO with a truncated or debilitating ZF (Fig. 2C, S2D), though both mutants were defective in supporting TNF α -induced kinase activity (Fig. S2E), consistent with data reported by Makris *et al.* (Makris et al., 2002). Thus, the ZF of NEMO appears to be largely dispensable for the activation of the IKK complex by IL-1 β and LPS in fibroblasts, reflecting stimulus-specific requirements for IKK activation.

If the ZF were necessary for recruiting the IKK complex to I κ Bs, a defect in I κ B α phosphorylation and degradation and subsequent NF κ B activation in cells expressing ZF-mutated NEMO would be anticipated. As expected, in NEMO^{-/-} cells expressing WT NEMO or a neutral M408S mutant, phosphorylation and degradation of I κ B α were induced by IL-1 β (Fig. 2D). However, in cells expressing NEMO with a truncated or debilitating ZF, IL-1 β stimulation triggered neither I κ B α phosphorylation nor degradation. Furthermore, NF κ B DNA binding activity induced by IL-1 β , LPS and TNF was defective with ZF mutants while it was strongly activated in WT and M408S expressing cells (Fig. 2E, S2F, S2G). The reduction in kinase activity measured in cells expressing truncated or C389/93S NEMO could not account for the observed defect in NF κ B activation, as similarly low kinase activities in WT cells (elicited by lower stimulus concentrations) allowed for detection of strong NF κ B DNA binding ability (Fig. S2H). These data are consistent with

results obtained with constitutively active IKK2 and further indicate that NEMO does indeed play a role in NF κ B activation that is distinct from its function in activating the IKK complex, most likely by facilitating the recruitment of I κ Bs to the IKK complex.

NEMO forms a complex with IKK β and I κ B α

NEMO's apparent role as a specificity factor for IKK may be mediated by allostery altering the catalytic specificity of the enzyme, or by functioning as a scaffold tethering I κ B substrates towards the catalytic site. Given that *in vitro* kinase assays did not reveal differences in catalytic activity we hypothesized that NEMO functions as a recruitment scaffold by enhancing the IKK-I κ B interaction through an N-terminal interaction with IKK β , and a C-terminal interaction with I κ B α (Fig. 3A). To test this hypothesis, I κ B α was immunoprecipitated and its interaction with IKK β and NEMO was analyzed by immunoblotting (Fig. 3B). A strong interaction between I κ B and IKK could be detected in the presence of WT NEMO but not in its absence. Deletion of the ZF abolished binding. The interaction was dependent on IKK β , as the interaction of I κ B with WT NEMO was reduced in the absence of IKK β or when an N-terminally truncated NEMO, which lacks the IKK β binding site, was used. Comparable results were obtained when NEMO was immunoprecipitated (Fig. S3). Together, these data indicate that NEMO interacts with I κ B α , that the ZF is required for this interaction, and that the interaction is strengthened in the presence of IKK β , suggesting the existence of a I κ B:IKK:NEMO complex.

In a functional assay, in which steady-state expression of I κ B α was analyzed in the presence of small amounts of IKK β EE, reduced levels of I κ B α could only be detected when WT NEMO was cotransfected, but not when N- and C-terminally truncated NEMO was expressed, further suggesting that NEMO indeed enhances I κ B α turnover by means of complex formation with I κ B α and IKK β (Fig. 3C).

The N-terminal 54 amino acids of I κ B α are known to be sufficient for phosphorylation by IKK β (Fig. 3D) (Wu and Ghosh, 2003). As NEMO appears to be important for targeting IKK β to I κ B α , I κ B β and I κ B ϵ , we hypothesized that a region conserved in canonical I κ Bs would mediate the interaction with NEMO. Most mutations of conserved residues in I κ B α showed no defects in phosphorylation and degradation upon stimulation with IL-1 β (data not shown). However, mutation of negatively charged residues D27 and D28 (corresponding to D14 and E15 in I κ B β) to positively charged arginines resulted in a strong reduction of inducible phosphorylation and degradation upon stimulation with IL-1 β (Fig. 3E), indicating that these amino acids are critical for phosphorylation by IKK β in cells. IKK β EE-induced phosphorylation of both the full-length and 1–54 I κ B D27/28R mutants was comparable with WT I κ B α in *in vitro* kinase assays (Fig. 3F), indicating that the consensus phosphorylation site for IKK β was not disrupted by the mutation. Instead, the *in vivo* defect in phosphorylation may be due to impaired recruitment by NEMO as the D27/28R I κ B α mutation weakened I κ B α 's interaction with NEMO and IKK2 (Fig. 3G). Together, these data indicate that in cells, NEMO forms a complex with I κ B α and IKK β and that amino acids D27 and D28 in the N-terminus of I κ B α are critical for complex formation.

To test the interaction between NEMO and I κ B α more directly, we produced highly purified recombinant, bacterially expressed NEMO and I κ B α and performed gel filtration analysis. As shown in Figure 3H, free I κ B α was detected in the low molecular weight fractions 26–35. In the presence of full-length NEMO I κ B α was also present in NEMO-containing high molecular weight fractions (13–18). In contrast, no change in the elution profile of I κ B α was detected in the presence of a C-terminal NEMO deletion mutant (lower panel). These data are indicative of a direct interaction between NEMO and I κ B α that depends on NEMO's C-terminus.

NEMO functions as a scaffold for IKK β

A hallmark of scaffold proteins is a non-monotonic dose response curve: increasing amounts of scaffold allow for increased complex formation, but when the scaffold concentration exceeds that of the kinase or substrate whose interaction it coordinates, then the excess will inhibit the formation of the full complex, by instead favoring the formation of many incomplete subcomplexes, an effect referred to as "combinatorial inhibition" (Ferrell, 2000; Levchenko et al., 2000). Accordingly, computational simulations of a mathematical model for the formation of the I κ B-NEMO-IKK complex (Supplementary Methods) showed increased complex formation when NEMO amounts are increased within a substoichiometric regime, but reduced functional complexes within higher regime (Fig. 4A). To test this experimentally, we transfected 293T cells with increasing amounts of NEMO and limiting amounts of IKK β EE. Expression of small to intermediate amounts of NEMO led to a dose-dependent increase of I κ B phosphorylation and reduced levels of total I κ B α expression (Fig. 4B and quantification Fig. 4C) caused by intrinsic IKK β EE activity. Strikingly, high overexpression resulted in reduced phosphorylation of I κ B α and increased I κ B α levels. Expression of NEMO mutants that only interacted with either IKK β (NEMO Δ C25) or I κ B α (NEMO Δ N) had no effect. The kinase activity, assayed *in vitro*, remained unchanged throughout all NEMO expression levels (Fig. 4D and S4). Thus, in the context of physical interactions delineated in Fig. 3B-H, the functional characteristics described in Fig. 4A-B support the conclusion that NEMO functions as a specificity scaffold that recruits classical I κ Bs to IKK.

Throughout these studies of NEMO's role as a specificity factor *in vivo*, we failed to observe such a function *in vitro*. We considered the explanation that the substrate availability/concentration in cells is lower than in *in vitro* kinase assay reaction conditions, in which substrate is supplied in excess to ensure sensitivity and linear dose responses. To test this hypothesis we attempted to mimic *in vivo* conditions by performing the kinase reaction in the presence of high concentration of non-specific competitor protein (BSA) and limiting concentrations of substrate. Using these conditions, I κ B α phosphorylation was stronger and occurred with faster kinetics in the presence than in the absence of NEMO (Fig. 4E). In contrast, ZF-deleted NEMO failed to enhance I κ B α phosphorylation. Similarly NEMO had no effect on phosphorylation of I κ B α DR, which is phosphorylation defective *in vivo*. These data further support the notion that NEMO acts as a scaffold for IKK β likely by enhancing the local concentration of I κ B to allow for its more efficient phosphorylation.

NEMO directs IKK β activity away from alternative substrates

IKK β is a pleiotropic kinase that is known to phosphorylate numerous alternative substrates *in vivo*, in addition to I κ B α . To analyze the potential effect of the scaffolding function of NEMO in this *in vivo* scenario we constructed an *in silico* model for I κ B phosphorylation, in which IKK β can bind to and phosphorylate I κ Bs or alternative substrates (Fig. 5A). Akin to our experimental results (Fig. 4E), model simulations suggested that in the absence of alternative substrates (i.e. *in vitro*) the ZF-dependent NEMO scaffold function would have little effect on phosphorylation of I κ B, while in their presence (i.e. *in vivo*), efficient phosphorylation of I κ B may only occur in the presence of WT but not ZF-mutant NEMO (Fig. 5B, left panel). In contrast, NEMO's scaffolding function was predicted to restrict the phosphorylation of alternate substrates with the ZF mutant NEMO leading to the hyperphosphorylation of alternative IKK β substrates (Fig. 5B, right panel).

To test this prediction experimentally, we analyzed steady-state phosphorylation of RelA/p65 Ser536, a well-established alternative target of IKK β . Only low levels of p65 were phosphorylated in NEMO-deficient cells, but IKK β EE expression greatly enhanced phosphorylation levels (Fig. 5C). Strikingly, expression of WT NEMO resulted in a strong

reduction of phosphorylated p65, while ZF-mutated NEMO showed similar p-p65 levels as the parental NEMO-deficient IKK β EE cells, indicating that in contrast to I κ B α , p65 is a NEMO-independent substrate. Indeed, in kinase assays performed in the presence of competitor protein and limiting amounts of substrate to reflect *in vivo* conditions, NEMO had no effect on the phosphorylation of p65 or p105, while I κ B α phosphorylation was strongly enhanced by the addition of NEMO (Fig. 5D and 5E). In contrast, without competitor, phosphorylation of I κ B α , p65 and p105 was unaffected by NEMO (Fig. 5E and S5C). These data not only demonstrate that NEMO does not affect IKK β kinase activity per se, but that it specifically channels IKK β kinase activity to I κ B α in conditions of low substrate abundance.

Next we asked whether we could observe similar substrate competition in the context of stimulated cells. As expected, IL-1 β stimulation rapidly induced I κ B α phosphorylation in NEMO-deficient cells reconstituted with WT NEMO, (Fig. 6A). No I κ B α phosphorylation was detectable in the presence of ZF-mutant NEMO but instead alternative IKK β substrates, p65 and p105, were strongly phosphorylated. Similar results were obtained upon stimulation with LPS (Fig. S6A). Phosphorylation of p65 and p105 was indeed caused by IKK β as treatment with an IKK β -specific inhibitor abolished phosphorylation (Fig. S6B). Despite hyperphosphorylation of p65 and p105 we did not detect measurable levels of NF κ B activity (Fig. 2E and data not shown). These data confirm that NEMO not only enhances phosphorylation of I κ Bs but also restricts the phosphorylation of alternative substrates.

We next addressed the implicit hypothesis that I κ B and alternative substrates are effectively competing *in vivo* for limited enzyme activity. Using cells that lack the I κ B substrates (*ikba*^{-/-} *β*^{-/-} *ε*^{-/-}) phosphorylation of both, p65 and p105 was strongly induced as early as 5 min post-IL-1 β stimulation while it was barely induced in WT cells (Fig. 6B). These data suggest that NEMO's role as a specificity factor is dependent on the availability of I κ B substrates, further supporting a role of NEMO in acting as a scaffold/tethering factor to direct IKKs activity specifically to I κ Bs.

Recent studies have shown that I κ B α phosphorylation and degradation are not required for IKK β -induced autophagy, suggesting the involvement of alternative IKK β substrates (Comb et al., 2011; Criollo et al., 2010). Our model of NEMO as a specificity factor for I κ Bs that restricts the phosphorylation of alternative IKK β substrates would predict that autophagy may be hyperactivated in cells that express ZF-debilitated NEMO. Indeed, when, ZF-deleted NEMO was expressed along with IKK β EE the number of cells that stained positive for the autophagy marker LC3 was significantly enhanced over that of WT NEMO controls (Fig. 6C). Concomitantly, phosphorylation of p70S6K, a marker for mTOR activity, was strongly reduced, while the upstream AMPK was hyperphosphorylated in cells expressing the ZF mutant NEMO (Fig. 6D), indicating that the signaling required for the induction of autophagy is hyperactivated by constitutively active IKK β when NEMO's I κ B targeting function is lost. Similarly, starvation increased the number of LC3 positive cells harboring a ZF-deleted NEMO (Fig. 6E) despite comparable levels of NEMO-associated IKK kinase activity (Fig. S6C). These data further show that autophagy is hyperactivated when IKK β loses its ability to phosphorylate I κ Bs, but instead hyperphosphorylates alternative substrates.

Discussion

We have presented several lines of evidence that NEMO plays an essential role in targeting IKK to the I κ B-NF κ B signaling module. Previous studies focused on NEMO's essential role in the activation of IKK via its ability to bind ubiquitin chains, which are a hallmark of inflammatory signaling by receptors of the TNFR and TLR/IL1R superfamilies. Using a

constitutively active IKK variant (Fig. 1) and identifying a specific mutation in NEMO (Fig. 2), we were able to distinguish between these two essential functions in activation and targeting. Physical interaction studies indicated that IKK-I κ B interactions are enhanced by NEMO, which interacts not only with IKK through its N-terminus (May et al., 2000; Mercurio et al., 1999) but may also form a stable complex with I κ B α via its C-terminus (Fig. 3). Using combined *in silico* kinetic modeling and *in vivo* experimental analysis we showed that the dose-response characteristics of NEMO are indeed consistent with bivalent interactions (Fig. 4) that support a scaffolding model for NEMO. Consistent with such a model, NEMO enhances I κ B phosphorylation in cells, and in *in vitro* conditions in which alternative substrates are abundant (Fig. 5). NEMO reduces alternate substrate phosphorylation (Fig. 6), and channels IKK activity specifically to I κ Bs; it therefore not only sensitizes the inflammatory pathway but may also increase its responsiveness to transient and dynamically regulated IKK signals (Cheong et al., 2006; Werner et al., 2005).

NF κ B activation occurs over a wide dynamic range. In the cyclin dependent kinase system, alternative substrates are thought to function as competitive inhibitors for specific phosphorylation (Kim and Ferrell, 2007). The resulting ultra-sensitivity renders the pathway insensitive to weak signals and responsive only to high levels of stimulus. The role of NEMO may thus be particularly important at low levels of stimulus as it counteracts the ultra-sensitivity brought by an abundance of alternative substrates. However, when IKK is highly activated NEMO's scaffolding function may be less critical. This may in part explain why Huang et al. (Huang et al., 2002) did not observe a strong defect in NF κ B activation in a ZF mutant B-cell line in response to high doses of LPS.

We show a direct interaction between recombinant purified NEMO and I κ B α (Fig. 3H). Our co-immunoprecipitation experiments suggest that the NEMO-I κ B α interaction is strengthened by IKK β (Fig. 3B), suggesting a stable ternary complex in which the N-terminus of NEMO binds to IKK while its C-terminus facilitates interaction with I κ B α , and IKK β itself interacts with the C-terminus of I κ B α through its ULD-SDD domains (Xu et al., 2011). Interestingly, this interaction appears to be important for IKKs specificity. Our data suggest that the N-terminal aspartic acids D27/28 in I κ B α are also critical for the efficient phosphorylation of I κ B α on S32/36 *in vivo*, while its ability to be phosphorylated by IKK β remains intact *in vitro*. Whether NEMO directly interacts with the I κ B α N-terminus or whether the N-terminal aspartic acids are participating in binding to IKK to form the functional ternary complex remains to be determined. However, our data support the function of NEMO as a scaffold that enhances the local concentration of I κ B α to allow for its specific and rapid phosphorylation.

Our work not only adds to our understanding of NEMO's biological function it also provides a framework for understanding IKK as a pleiotropic signal transducer that is involved in numerous biological processes and is capable of stimulus-specific phosphorylation of specific substrates. Although IKK's name suggests specificity for I κ B phosphorylation, it is NEMO that determines its substrate specificity and function within the inflammatory pathway. Akin to how the yeast MAPK Ste11p mediates distinct signaling axes responsive to mating pheromone or hyper-osmolarity depending on its association with scaffold proteins Ste5p or Pbs2p respectively (Engstrom et al., 2010; Schwartz and Madhani, 2004; van Drogen and Peter, 2002), NEMO defines the inflammatory signaling axis mediated by IKK, owing to its multivalent interactions with ubiquitin chains, IKK, and I κ B. We would expect that other scaffolds might be identified for IKK's alternate functions in autophagy or insulin signaling. Such scaffolds may either be similarly multivalent, capable of replacing NEMO and thus insulating the pathway from inflammatory signaling, or they may be bivalent to function with NEMO to connect IKK to other upstream activation pathways or target IKK to other downstream substrates. The latter scenarios would provide

for crosstalk with the inflammatory signaling axis, which may underlie the pleiotropic functions of inflammation itself. Related, it is not known whether the IKK interacting proteins RAP1 or ELKS, which are essential for phosphorylation of p65 (Teo et al., 2010) or activation by genotoxic stress (Wu et al., 2010), respectively, function with NEMO or in its stead. The use of scaffolds to direct IKK's target specificity constitutes a modular strategy to facilitate signaling specificity while allowing for signaling crosstalk within this regulatory hub.

The $\Delta C25$ NEMO mutant described here resembles NEMO expressed in some patients with incontinentia pigmenti (IP) as a result of a frameshift mutation (Makris et al., 2002). IP is an X-linked genetic disease thought to be caused in most part by inactivation of NF κ B signaling and hypersensitivity of NEMO-deficient cells to TNF-induced apoptosis (Courtois and Israel, 2011). Interestingly, in IP mouse models an increase of inflammatory cytokines including TNF and IL-1 β could be observed in the epidermis at the early onset of the disease (Makris et al., 2000; Nenci et al., 2006; Pasparakis et al., 2002). Hyperactivation of autophagy reported here might provide an explanation for this disease phenotype as autophagy has recently been implicated to positively contribute to the biogenesis and secretion of inflammatory cytokines such as IL-1 β (Dupont et al., 2011).

To harness the potential of the pleiotropic IKK signal transducer as a drug target in numerous types of inflammatory diseases, diabetes and cancers, it is critical to understand how its activity is directed to different signaling axes and cellular functions, and the degree to which these are insulated from or connected with each other. The present work identifies NEMO as a key molecule in this systems behavior and provides a framework for future investigations.

Experimental Procedures

Cell culture and stimulations

Immortalized NEMO-deficient MEFs were generated via the 3T3 protocol from embryos derived from NEMO^{-/-} mice (Rudolph et al., 2000). I κ B α ^{-/-} β ^{-/-} ϵ ^{-/-} cells and I κ B α ^{-/-} cells were described previously (Basak et al., 2007). 3T3 cells were reconstituted by retroviral transduction with WT or mutant pBABE.mNEMO.puro, pBABE.I κ B α .puro constructs, and/or with pBABE.IKK β EE.hygro or empty vector controls. Cells were selected with puromycin Hydrochlorid (Sigma) and hygromycin B (Invitrogen), respectively, and expression of the stably expressed constructs was verified by western blotting. Cells were stimulated with recombinant murine TNF α (Roche), LPS (Sigma), or murine IL-1 β (R&D).

Expression and purification of recombinant NEMO and I κ B α

His-tagged human recombinant full-length or 1–319 truncated human NEMO was cloned into pET29 expression vector. pET29.hNEMO WT or 1–319 and pET15.I κ B α were transformed into BL21 cells. Expression was induced with 0.25 mM IPTG at room temperature and upon sonication proteins were purified in a buffer containing 50 mM Tris, pH 7.5, 300 mM NaCl, 10% Glycerol, 10 mM Imidazole, 25 μ M ZnSO₄ (for WT NEMO) using Ni-NTA beads. Proteins were eluted in buffer containing 250 mM Imidazole and dialyzed.

Size exclusion chromatography

For size exclusion chromatography individual proteins were mixed with each other at a ratio of 1:1 and incubated at room temperature for 1hr to form complexes prior size exclusion chromatography. 150 μ l of each sample was loaded onto a Superose 6 10/300 GL column

(GE Healthcare) pre-equilibrated with 25 mM Tris pH 7.5, 150 mM NaCl, 5% Glycerol, 2 mM DTT and 40 μ M ZnSO₄ and resolved at a flow rate of 0.5 ml/min on an AkTA (GE Healthcare) automated liquid chromatography system. 0.5 ml size fractions were collected and an equal volume aliquot of each fraction was analyzed by Western blotting using relevant antibodies indicated in the respective figures.

Gel-Shift assay and IKK kinase assay

Gel-shift assays were performed as previously described (Basak et al., 2007). Briefly, nuclear extracts were incubated with ³²P-labeled 38 bp spanning double-stranded oligonucleotides containing 2 consensus κ B sites at room temperature for 20 min prior to complex separation on a nondenaturing acrylamide gel. Bands were visualized by autoradiography and quantified using ImageQuant software. *In vitro* IKK kinase assays were performed as described previously (Werner et al., 2005). The IKK complex was immunoprecipitated from cytoplasmic extracts using a NEMO specific antibody (BD or Santa Cruz Biotechnology) and Protein A-sepharose beads. In NEMO deficient cells IKK kinase complexes were precipitated using an IKK α antibody (Santa Cruz Biotechnology) or HA antibody (Covance) to pull down HA-tagged IKK β . Beads were subjected to *in vitro* kinase reaction containing ³²P-ATP and 1 μ g GST-I κ B α ₁₋₅₄, GST-I κ B α ₁₋₅₄ D27/28R, full-length wild-type or D27/28R His-I κ B α , full-length p105 or GST-p65_{AD} as substrates. For competitor experiments 10 μ g BSA and 50 ng of substrate and indicated amounts of recombinant wild-type or 1–319 hNEMO were added to the kinase reaction. Upon incubation at 30°C for indicated time, reactions were stopped by boiling samples in SDS sample buffer. Proteins were resolved by SDS-PAGE and visualized by autoradiography or western blotting.

Coimmunoprecipitation and Western blotting

For Western blot analysis, whole-cell extracts were prepared using RIPA buffer supplemented with PMSF, DTT, and phosphatase inhibitors. Samples were normalized for equal amounts of proteins using a Bradford assay (Biorad). Phospho-specific antibodies to I κ B α (S32/36) p65 (S536), p105 (S933), p-AMPK (T172) and AMPK, p-p70 S6 Kinase (T389) and p70 S6 Kinase were from Cell signaling. For coimmunoprecipitation experiments, 293T cells were transfected with indicated amounts of pcMyc-NEMO, pcFlag-I κ B α and pcHA-IKK β or empty vector. Total amounts of DNA used for transfections were normalized with empty vector. Cells were lysed in buffer containing 10 mM HEPES-KOH pH 7.9, 250 mM NaCl, 1 mM EDTA, 0.5% NP-40, 0.2% Tween 20, 1 mM DTT, 1 mM PMSF and 10 μ M MG132. Lysates were precleared with protein A/G sepharose beads followed by immunoprecipitation with anti-Myc (Roche), anti-HA (Covance) or anti-Flag (Sigma) antibody for 2h. Complexes were collected by addition of 10 μ l protein A/G Sepharose for 2h followed by extensive washing in lysis buffer at 37°C. Samples were analyzed on immunoblots probed with indicated antibodies.

Microscopy

Cells were grown on poly-L lysine-coated glass cover slips and where indicated treated with HBSS for starvation. Cells were fixed with 4% formaldehyde for 15 min, incubated with methanol at -20°C for 10 min followed by blocking with 10% normal goat serum for 1h. Anti-LC3A/B antibody (Cell Signaling) was used for scoring cells undergoing autophagy. Goat-anti-rabbit Alexa-fluor 488 (Invitrogen) was used as secondary antibody. Nuclei were counterstained with Hoechst. Images were taken on a Zeiss Axio Observer Z1 microscope. For quantification at least 50 cells were counted in three independent experiments. Statistical significance was tested using two-sided student's T-test.

Highlights

- Constitutively active IKK β is unable to activate NF κ B in the absence of NEMO
- NEMO directly interacts with I κ B α via its zinc finger
- NEMO functions as a scaffold to recruit I κ B α to IKK β
- Without NEMO, active IKK β hyper-activates alternative substrates and Autophagy

Supplementary Material

Refer to Web version on PubMed Central for supplementary material.

Acknowledgments

BS is a Leukemia and Lymphoma Society fellow, and MB is a Cancer Research Institute fellow. The work was supported by NCI RO1 grant CA141722 and NIGMS P50 GM085763.

References

- Amit S, Hatzubai A, Birman Y, Andersen JS, Ben-Shushan E, Mann M, Ben-Neriah Y, Alkalay I. Axin-mediated CKI phosphorylation of beta-catenin at Ser 45: a molecular switch for the Wnt pathway. *Genes & development*. 2002; 16:1066–1076. [PubMed: 12000790]
- Basak S, Kim H, Kearns JD, Tergaonkar V, O'Dea E, Werner SL, Benedict CA, Ware CF, Ghosh G, Verma IM, Hoffmann A. A fourth I κ B protein within the NF- κ B signaling module. *Cell*. 2007; 128:369–381. [PubMed: 17254973]
- Bhattacharyya RP, Remenyi A, Yeh BJ, Lim WA. Domains, motifs, and scaffolds: the role of modular interactions in the evolution and wiring of cell signaling circuits. *Annu Rev Biochem*. 2006; 75:655–680. [PubMed: 16756506]
- Burack WR, Shaw AS. Signal transduction: hanging on a scaffold. *Curr Opin Cell Biol*. 2000; 12:211–216. [PubMed: 10712921]
- Chariot A. The NF- κ B-independent functions of IKK subunits in immunity and cancer. *Trends Cell Biol*. 2009; 19:404–413. [PubMed: 19648011]
- Cheong R, Bergmann A, Werner SL, Regal J, Hoffmann A, Levchenko A. Transient I κ B kinase activity mediates temporal NF- κ B dynamics in response to a wide range of tumor necrosis factor- α doses. *The Journal of biological chemistry*. 2006; 281:2945–2950. [PubMed: 16321974]
- Comb WC, Cogswell P, Sitcheran R, Baldwin AS. IKK-dependent, NF- κ B-independent control of autophagic gene expression. *Oncogene*. 2011; 30:1727–1732. [PubMed: 21151171]
- Courtois G, Israel A. IKK regulation and human genetics. *Curr Top Microbiol Immunol*. 2011; 349:73–95. [PubMed: 20845108]
- Criollo A, Senovilla L, Authier H, Maiuri MC, Morselli E, Vitale I, Kepp O, Tasdemir E, Galluzzi L, Shen S, et al. The IKK complex contributes to the induction of autophagy. *EMBO J*. 2010; 29:619–631. [PubMed: 19959994]
- Dueber JE, Yeh BJ, Chak K, Lim WA. Reprogramming control of an allosteric signaling switch through modular recombination. *Science*. 2003; 301:1904–1908. [PubMed: 14512628]
- Dupont N, Jiang S, Pilli M, Ornatowski W, Bhattacharya D, Deretic V. Autophagy-based unconventional secretory pathway for extracellular delivery of IL-1 β . *EMBO J*. 2011; 30:4701–4711. [PubMed: 22068051]
- Engstrom W, Ward A, Moorwood K. The role of scaffold proteins in JNK signalling. *Cell Prolif*. 2010; 43:56–66. [PubMed: 19922489]
- Ferrell JE Jr. What do scaffold proteins really do? *Sci STKE*. 2000; 2000:pe1. [PubMed: 11752612]

- Gao Z, Hwang D, Bataille F, Lefevre M, York D, Quon MJ, Ye J. Serine phosphorylation of insulin receptor substrate 1 by inhibitor kappa B kinase complex. *The Journal of biological chemistry*. 2002; 277:48115–48121. [PubMed: 12351658]
- Hayden MS, Ghosh S. Shared principles in NF-kappaB signaling. *Cell*. 2008; 132:344–362. [PubMed: 18267068]
- Hoffmann A, Baltimore D. Circuitry of nuclear factor kappaB signaling. *Immunol Rev*. 2006; 210:171–186. [PubMed: 16623771]
- Huang TT, Feinberg SL, Suryanarayanan S, Miyamoto S. The zinc finger domain of NEMO is selectively required for NF-kappa B activation by UV radiation and topoisomerase inhibitors. *Mol Cell Biol*. 2002; 22:5813–5825. [PubMed: 12138192]
- Israel A. The IKK complex, a central regulator of NF-kappaB activation. *Cold Spring Harb Perspect Biol*. 2010; 2:a000158. [PubMed: 20300203]
- Kim SY, Ferrell JE Jr. Substrate competition as a source of ultrasensitivity in the inactivation of Wee1. *Cell*. 2007; 128:1133–1145. [PubMed: 17382882]
- Lamberti C, Lin KM, Yamamoto Y, Verma U, Verma IM, Byers S, Gaynor RB. Regulation of beta-catenin function by the IkappaB kinases. *The Journal of biological chemistry*. 2001; 276:42276–42286. [PubMed: 11527961]
- Laplantine E, Fontan E, Chiaravalli J, Lopez T, Lakisic G, Veron M, Agou F, Israel A. NEMO specifically recognizes K63-linked poly-ubiquitin chains through a new bipartite ubiquitin-binding domain. *EMBO J*. 2009; 28:2885–2895. [PubMed: 19763089]
- Lee DF, Kuo HP, Chen CT, Hsu JM, Chou CK, Wei Y, Sun HL, Li LY, Ping B, Huang WC, et al. IKK beta suppression of TSC1 links inflammation and tumor angiogenesis via the mTOR pathway. *Cell*. 2007; 130:440–455. [PubMed: 17693255]
- Levchenko A, Bruck J, Sternberg PW. Scaffold proteins may biphasically affect the levels of mitogen-activated protein kinase signaling and reduce its threshold properties. *Proc Natl Acad Sci U S A*. 2000; 97:5818–5823. [PubMed: 10823939]
- Makris C, Godfrey VL, Krahn-Senfleben G, Takahashi T, Roberts JL, Schwarz T, Feng L, Johnson RS, Karin M. Female mice heterozygous for IKK gamma/NEMO deficiencies develop a dermatopathy similar to the human X-linked disorder incontinentia pigmenti. *Molecular cell*. 2000; 5:969–979. [PubMed: 10911991]
- Makris C, Roberts JL, Karin M. The carboxyl-terminal region of IkappaB kinase gamma (IKKgamma) is required for full IKK activation. *Mol Cell Biol*. 2002; 22:6573–6581. [PubMed: 12192055]
- May MJ, D'Acquisto F, Madge LA, Glockner J, Pober JS, Ghosh S. Selective inhibition of NF-kappaB activation by a peptide that blocks the interaction of NEMO with the IkappaB kinase complex. *Science*. 2000; 289:1550–1554. [PubMed: 10968790]
- Mercurio F, Murray BW, Shevchenko A, Bennett BL, Young DB, Li JW, Pascual G, Motiwala A, Zhu H, Mann M, Manning AM. IkappaB kinase (IKK)-associated protein 1, a common component of the heterogeneous IKK complex. *Mol Cell Biol*. 1999; 19:1526–1538. [PubMed: 9891086]
- Nenci A, Huth M, Funteh A, Schmidt-Supprian M, Bloch W, Metzger D, Chambon P, Rajewsky K, Krieg T, Haase I, Pasparakis M. Skin lesion development in a mouse model of incontinentia pigmenti is triggered by NEMO deficiency in epidermal keratinocytes and requires TNF signaling. *Hum Mol Genet*. 2006; 15:531–542. [PubMed: 16399796]
- Pasparakis M, Courtois G, Hafner M, Schmidt-Supprian M, Nenci A, Toksoy A, Krampert M, Goebeler M, Gillitzer R, Israel A, et al. TNF-mediated inflammatory skin disease in mice with epidermis-specific deletion of IKK2. *Nature*. 2002; 417:861–866. [PubMed: 12075355]
- Rudolph D, Yeh WC, Wakeham A, Rudolph B, Nallainathan D, Potter J, Elia AJ, Mak TW. Severe liver degeneration and lack of NF-kappaB activation in NEMO/IKKgamma-deficient mice. *Genes & development*. 2000; 14:854–862. [PubMed: 10766741]
- Scheidereit C. IkappaB kinase complexes: gateways to NF-kappaB activation and transcription. *Oncogene*. 2006; 25:6685–6705. [PubMed: 17072322]
- Schwartz MA, Madhani HD. Principles of MAP kinase signaling specificity in *Saccharomyces cerevisiae*. *Annu Rev Genet*. 2004; 38:725–748. [PubMed: 15568991]

- Teo H, Ghosh S, Luesch H, Ghosh A, Wong ET, Malik N, Orth A, de Jesus P, Perry AS, Oliver JD, et al. Telomere-independent Rap1 is an IKK adaptor and regulates NF-kappaB-dependent gene expression. *Nat Cell Biol.* 2010; 12:758–767. [PubMed: 20622870]
- Ubersax JA, Ferrell JE Jr. Mechanisms of specificity in protein phosphorylation. *Nat Rev Mol Cell Biol.* 2007; 8:530–541. [PubMed: 17585314]
- van Drogen F, Peter M. MAP kinase cascades: scaffolding signal specificity. *Curr Biol.* 2002; 12:R53–R55. [PubMed: 11818078]
- Werner S, Barken D, Hoffmann A. Stimulus specificity of gene expression programs determined by temporal control of IKK activity. *Science.* 2005; 309:1857–1861. [PubMed: 16166517]
- Wu C, Ghosh S. Differential phosphorylation of the signal-responsive domain of I kappa B alpha and I kappa B beta by I kappa B kinases. *The Journal of biological chemistry.* 2003; 278:31980–31987. [PubMed: 12791687]
- Wu D, Pan W. GSK3: a multifaceted kinase in Wnt signaling. *Trends Biochem Sci.* 2010; 35:161–168. [PubMed: 19884009]
- Wu ZH, Wong ET, Shi Y, Niu J, Chen Z, Miyamoto S, Tergaonkar V. ATM- and NEMO-dependent ELKS ubiquitination coordinates TAK1-mediated IKK activation in response to genotoxic stress. *Molecular cell.* 2010; 40:75–86. [PubMed: 20932476]
- Xia Y, Padre RC, De Mendoza TH, Bottero V, Tergaonkar VB, Verma IM. Phosphorylation of p53 by IkappaB kinase 2 promotes its degradation by beta-TrCP. *Proc Natl Acad Sci U S A.* 2009; 106:2629–2634. [PubMed: 19196987]
- Xu G, Lo YC, Li Q, Napolitano G, Wu X, Jiang X, Dreano M, Karin M, Wu H. Crystal structure of inhibitor of kappaB kinase beta. *Nature.* 2011; 472:325–330. [PubMed: 21423167]
- Yang F, Yamashita J, Tang E, Wang HL, Guan K, Wang CY. The zinc finger mutation C417R of I-kappa B kinase gamma impairs lipopolysaccharide- and TNF-mediated NF-kappa B activation through inhibiting phosphorylation of the I-kappa B kinase beta activation loop. *J Immunol.* 2004; 172:2446–2452. [PubMed: 14764716]

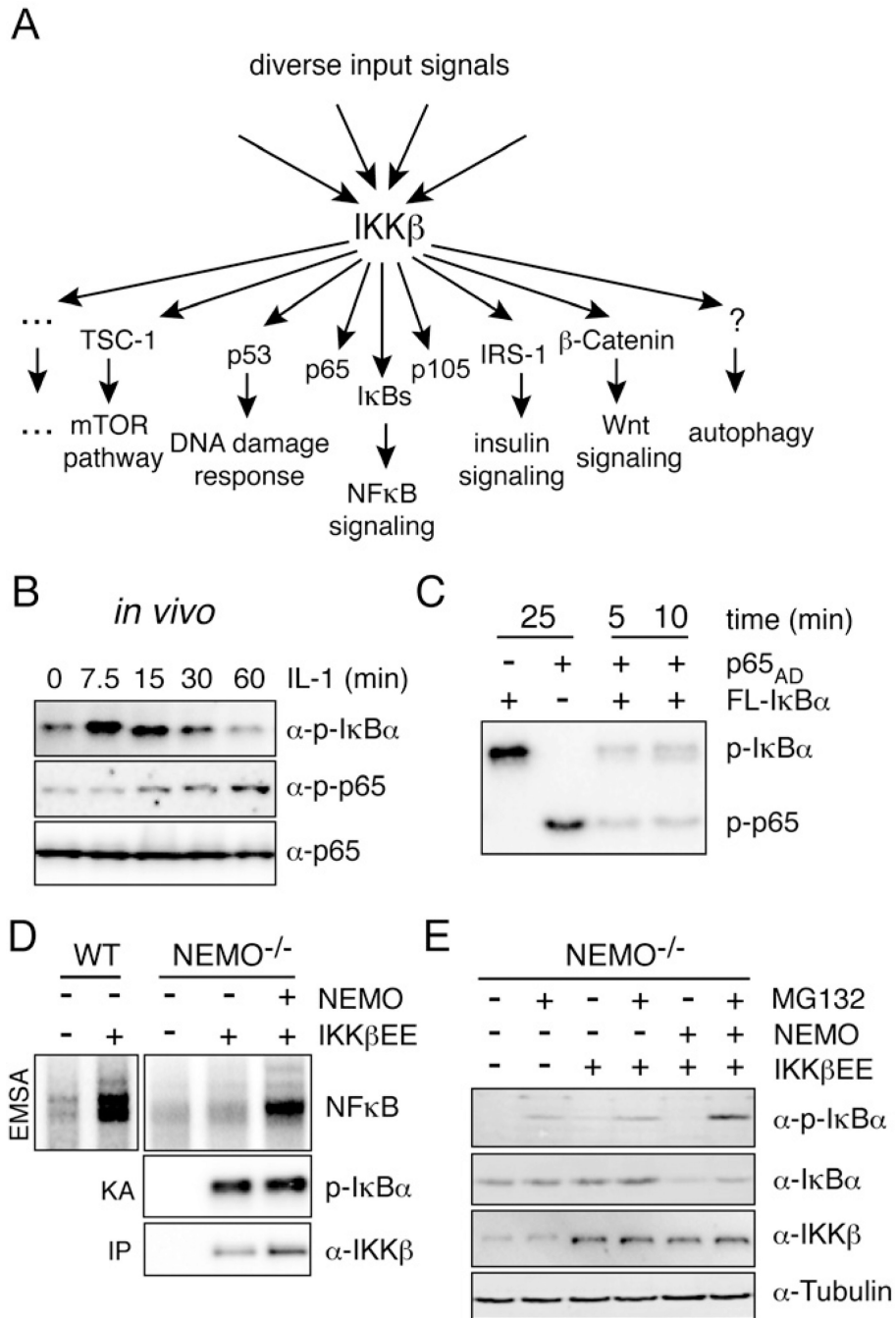


Figure 1. Constitutively active IKK β is not sufficient for NF κ B activation, but requires NEMO
(A) IKK is a pleiotropic transducer capable of phosphorylating many substrates involved in different biological functions. IKK β phosphorylates the tumor suppressor p53 at S362 and S366 to regulate its stability (Xia et al., 2009), the insulin Receptor (IR) substrate 1 (IRS-1) at S307 resulting in the termination of metabolic insulin signaling (Gao et al., 2002), the tumor suppressor Tuberous sclerosis 1 (TSC1) at S487 and S511 to activate the mTOR pathway, enhance angiogenesis and tumor development (Lee et al., 2007), β -catenin, a key molecule in Wnt signaling, as well as FOXO3a which acts downstream of growth factor signaling (PI3K/Akt) (Lamberti et al., 2001). Induction of autophagy depends on IKK β

kinase activity, the relevant substrates remain to be identified (Comb et al.; Criollo et al.). **(B)** Phosphorylation of I κ B α (S32/36) and p65 (S536) was measured in fibroblasts upon stimulation with 1 ng/ml IL-1 β . **(C)** *In vitro* activity of constitutively active HA-IKK β EE purified from transfected 293T cells was measured using FL-I κ B α or the activation domain of p65 (p65_{AD}) alone (25 min incubation), or mixed together. Time indicates kinase reaction time. **(D)** Steady-state NF κ B activity was measured by EMSA in NEMO deficient cells supplemented with indicated constructs and IKK kinase activity was determined in an *in vitro* kinase reaction using FL-I κ B α as substrate upon immunoprecipitation of IKK β with an HA antibody. **(E)** Western blot analysis of I κ B α phosphorylation and steady-state expression levels in indicated cells with or without MG132 treatment. See also Figure S1.

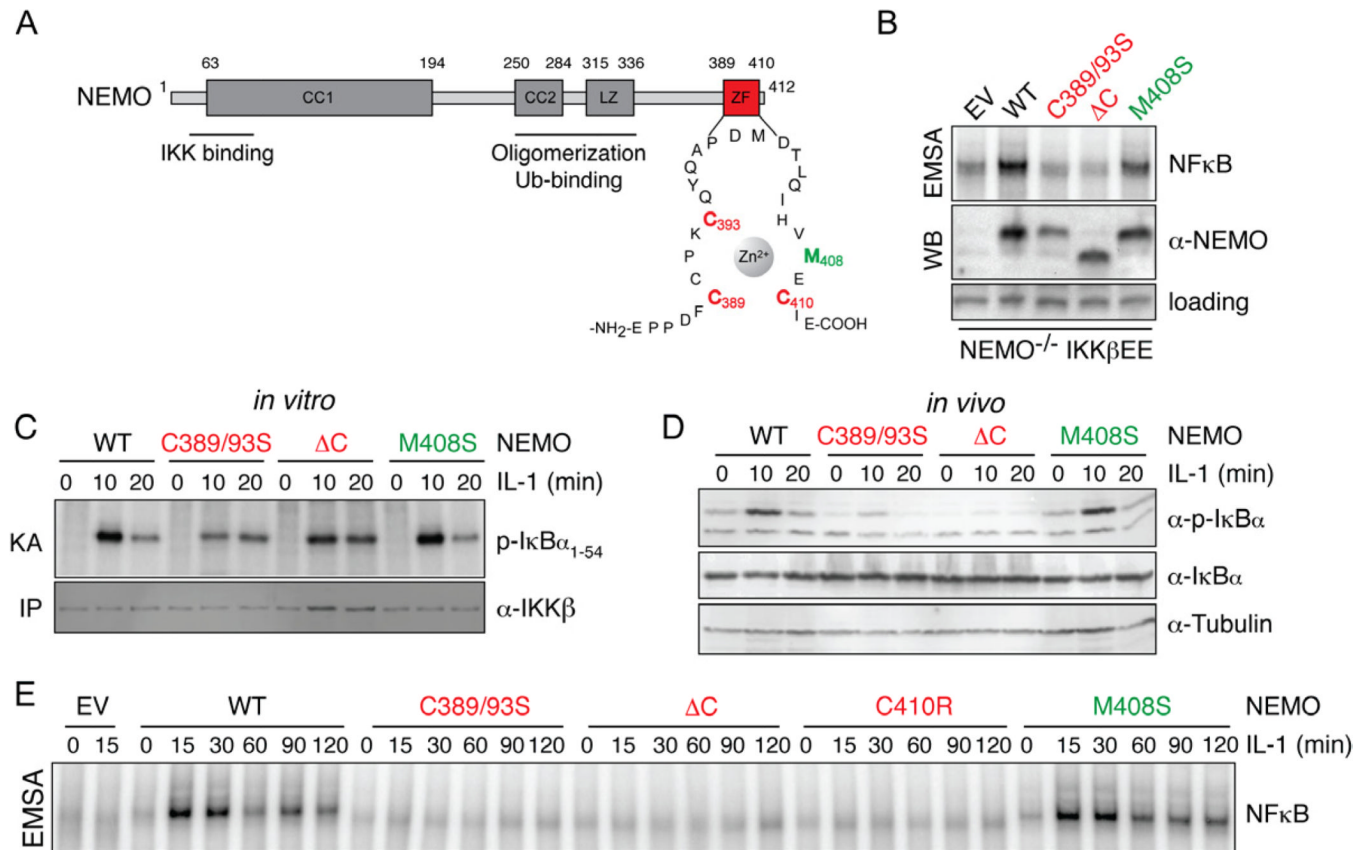


Figure 2. The Zinc-finger of NEMO is dispensable for IKK activation by IL-1 but necessary for NFκB DNA binding activity

(A) Domain structure of mouse NEMO. NEMO contains 2 coiled coil domains (CC1 and CC2), a leucine zipper (LZ) motif and a zinc finger (ZF). Mutations introduced into the NEMO ZF are highlighted in red and green. (B) NFκB activity (top) was measured in NEMO-deficient cells expressing IKKβEE and indicated NEMO constructs by EMSA. Expression levels of NEMO are shown below. (C) NEMO-associated kinase activity was determined in NEMO-deficient cells expressing indicated mutant NEMO in an *in vitro* IP-kinase assay upon stimulation with IL-1 for indicated times. (D) Western blot analysis of phosphorylation status and total levels of IκBα upon stimulation with IL-1. (E) NFκB DNA binding activity of NEMO deficient cells reconstituted with the indicated mutant NEMO constructs was measured by EMSA upon stimulation with IL-1 (10 ng/ml). See also Figure S2.

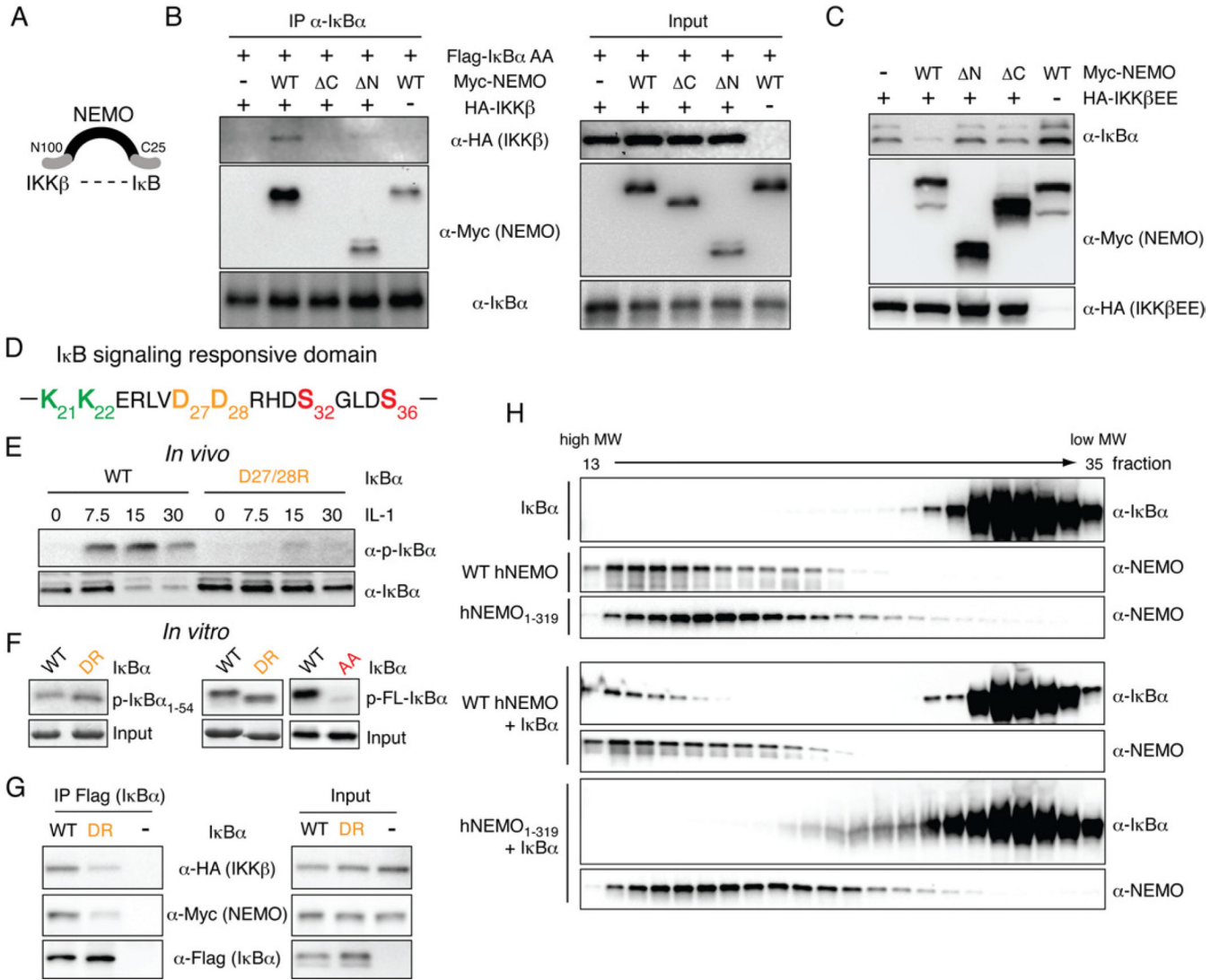


Figure 3. NEMO forms a complex with IKK β and I κ B α . (A) Schematic of a possible complex between NEMO, IKK β and I κ B α . The N-terminal 100 amino acids of NEMO facilitate interaction with IKK β , while the C-terminal ZF might allow for interaction with I κ B α . (B) NEMO interacts with I κ B α via its C-terminus. 293T cells were transfected with non-degradable Flag-I κ B α (Flag-I κ B α AA), HA-IKK β , and WT or mutant Myc-NEMO constructs. Left panel: Complexes were analyzed upon immunoprecipitation of I κ B α by western blotting using indicated antibodies. Right panel: Expression levels of inputs were analyzed in parallel. (C) The NEMO C-terminus is required for signaling to I κ B α . 293T cells were transfected with small amounts of IKK β EE together with indicated NEMO mutants and I κ B α steady-state levels were analyzed by western blotting. (D) Amino acid sequence of the I κ B α signaling responsive domain. Key amino acids discussed in the text are shown in color. (E) Phosphorylation and expression of WT and DR mutated I κ B α stably expressed in I κ B α -deficient cells was analyzed upon stimulation with IL-1 by western blotting. Loading was adjusted to similar I κ B α levels. (F) Phosphorylation of WT or DR mutant I κ B α by IKK β EE was analyzed in an *in vitro* kinase assay using wild-type or DR mutant GST-I κ B α ₁₋₅₄ (left panel) or FL-I κ B α (middle panel) or FL-I κ B α with S32/36 mutated to alanine (AA) to control for specificity. (G) Interaction

between WT and DR I κ B α with NEMO and IKK β was analyzed by immunoprecipitation of I κ B α with an α -Flag antibody from 293T cells followed by western blot analysis with indicated antibodies. **(H)** Gel filtration of recombinant FL-human I κ B α , wild-type or 1–319 truncated human NEMO. Proteins were mixed at a ratio of 1:1 prior to gel filtration. Fractions 13–35 were analyzed by western blotting. See also Figure S3).

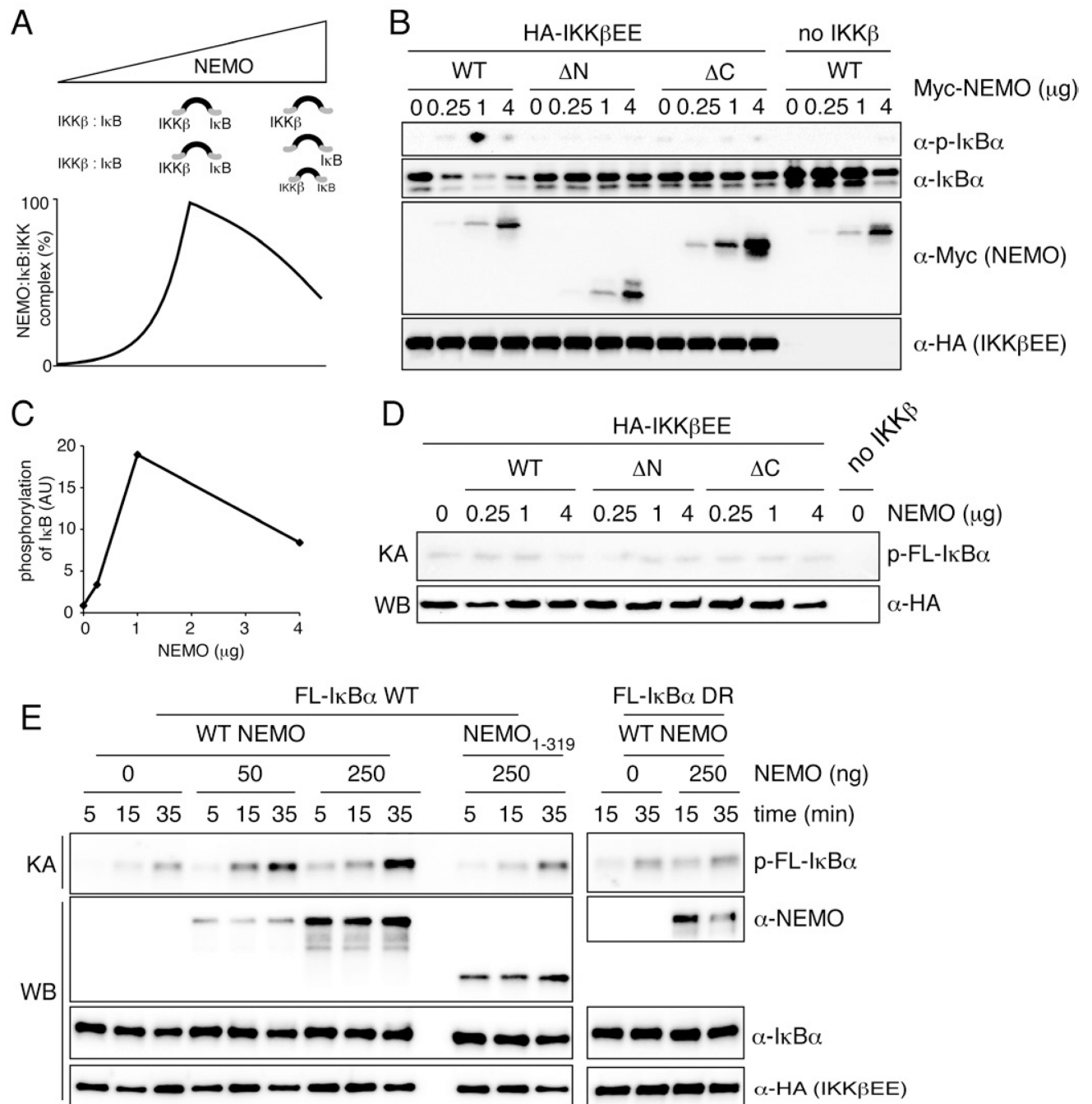


Figure 4. NEMO functions as a scaffold *in vivo* and *in vitro*

(A) Schematic and computational model simulation to illustrate combinatorial inhibition and its consequence on NEMO:I κ B:IKK complex formation and I κ B α phosphorylation. (B) 293T cells were transfected with HA-IKK β EE and increasing amounts of WT or mutant NEMO constructs. Levels of phosphorylated and total I κ B α were analyzed by western blotting. (C) Quantification of I κ B α phosphorylation in (B). p-I κ B α was normalized to total I κ B α expression. (D) *In vitro* kinase assay from 293T cells transfected with HA-IKK β EE and indicated amounts of WT or mutant NEMO constructs. FL-I κ B α was used as substrate. (E) *In vitro* kinase assay using HA-IKK β EE purified from transfected 293T cells using 50

ng of full-length wild-type or DR I κ B α as substrate in the presence of 10 μ g BSA as non-specific competitor. 50 or 250 ng recombinant human wild-type of 1- 319 NEMO were added to the reaction as indicated. Time indicates kinase reaction time. Inputs were analyzed by western blotting in parallel. See also Figure S4.

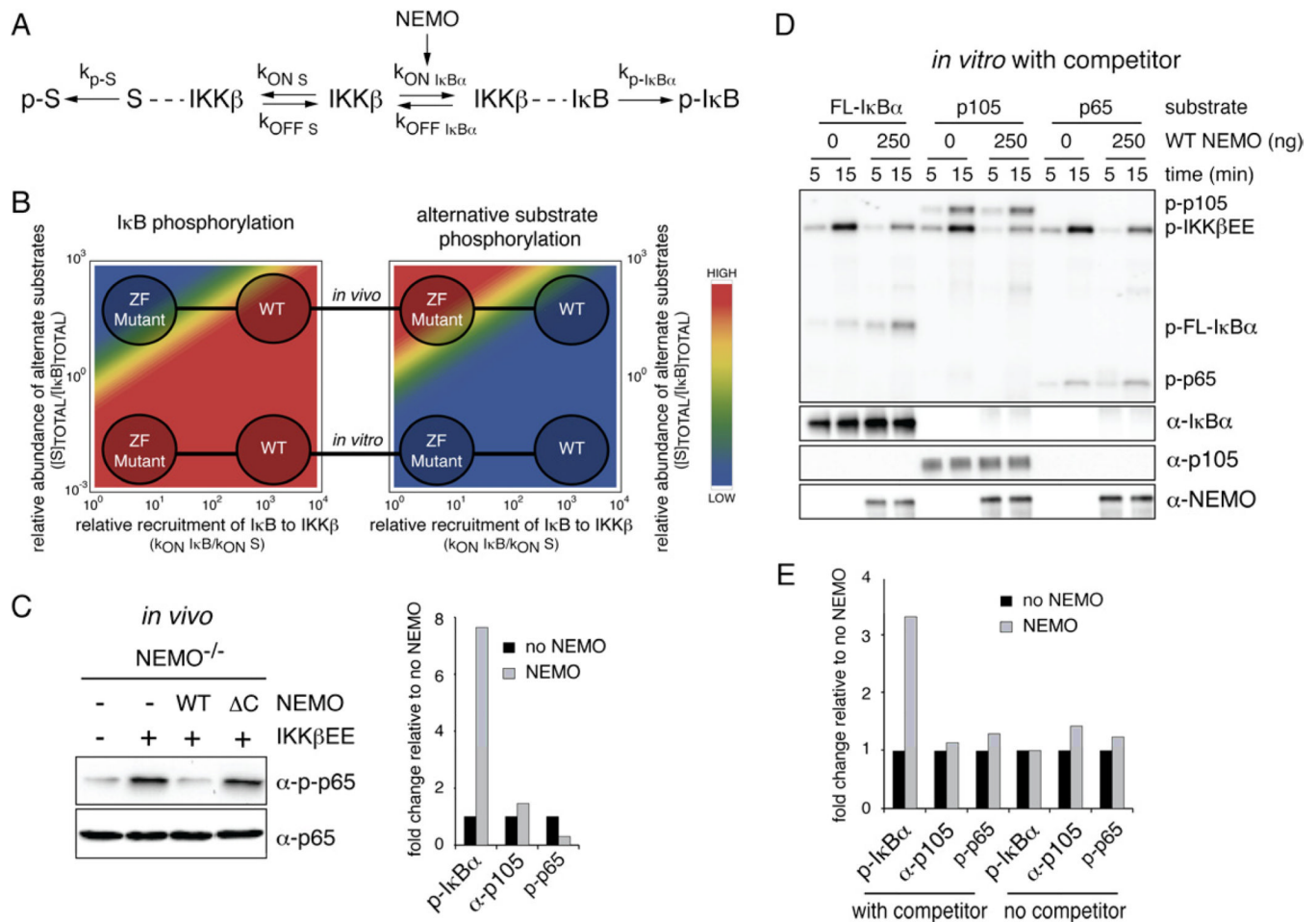


Figure 5. Substrate competition between IκBα, p65 and p105

(A) A model for competitive complex formation between IKK and IκB or alternative substrates. The presence of NEMO favors IKK:IκB complex formation, here modeled as NEMO-dependent increase of $k_{ON}I\kappa B$. (B) *In silico* model for IκB phosphorylation. Fraction of IKK bound to IκB and alternative substrate S (right and left respectively) as a function of the NEMO-induced stabilization of the IKK-IκB complex (x axis) and the relative concentration of alternative substrate S (y axis). The “*in vitro*” region is characterized by a very low ratio of S to IκB in contrast to the “*in vivo*” situation in which large amounts of alternative substrates S might be present. (C) NEMO-deficient cells were stably reconstituted with indicated vectors and phosphorylation of p65 at S536 was analyzed by western blotting. Quantification of steady-state phosphorylation of IκBα (Fig. 1E), p105 (S5A) and p65 (left panel). Phosphorylation signals were normalized to total protein and phosphorylation in the absence of NEMO was set to 1. (D) *In vitro* kinase assay of HA-IKKβEE using 50 ng of FL-IκBα, FL-p105 or p65AD as substrate in the presence of 10 mg BSA. Where indicated 250 ng recombinant WT NEMO were added. Inputs were analyzed by western blotting. (E) Quantification of phosphorylation of IκBα, p105 and p65 from kinase assays with competitor and limited substrate (5D) and without competitor and access substrate (55C) after a 15 minutes kinase reaction. Phosphorylation in the absence of NEMO was set to 1. See also Figure S5.

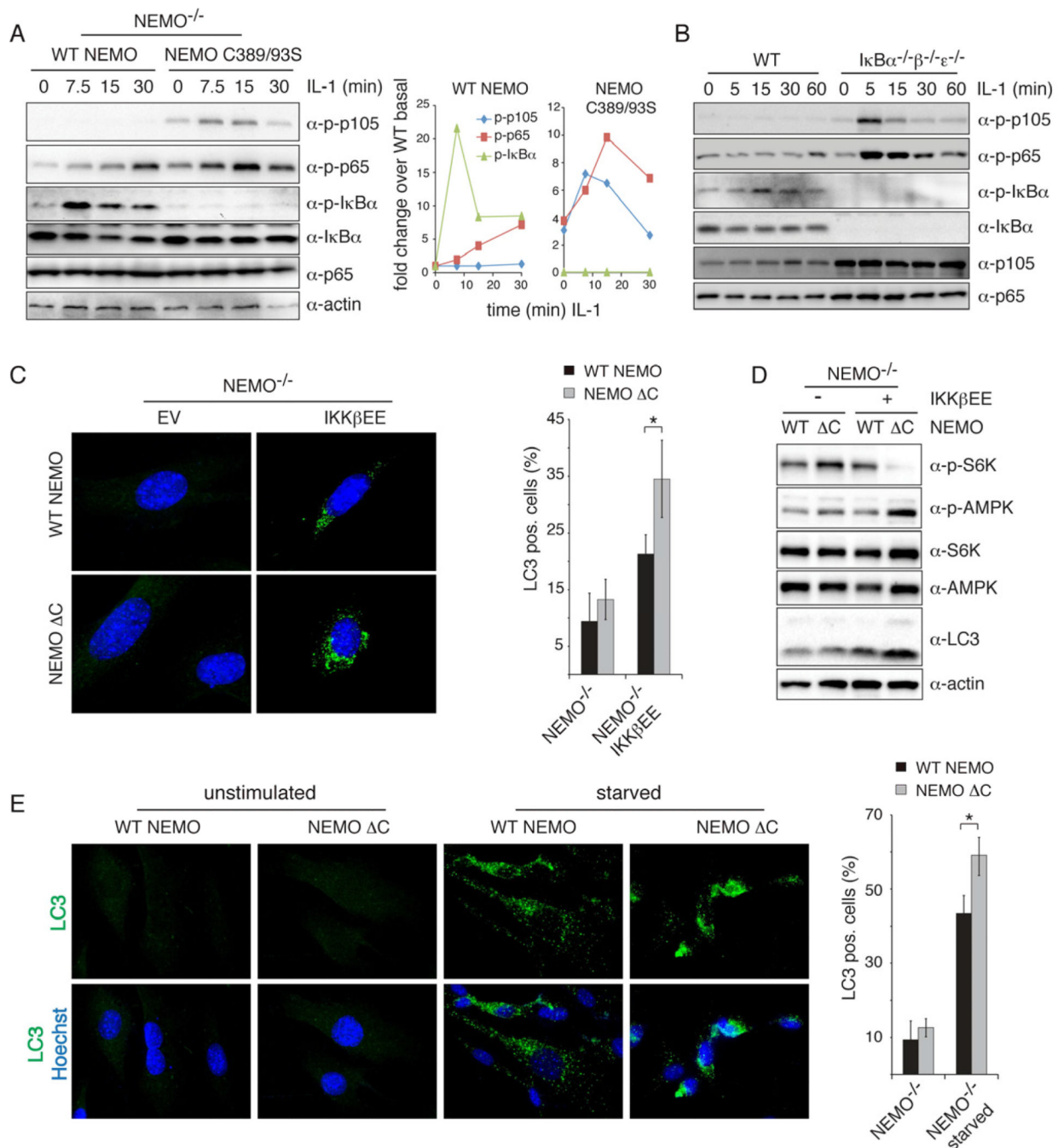


Figure 6. In the absence of NEMO scaffolding, IKKβ hyperphosphorylates alternative substrates and hyperactivates autophagy

(A) Phosphorylation of p105 (S933), p65 (S536) and IκBα (S32) was measured in NEMO-deficient cells reconstituted with WT or C389/93S mutant NEMO upon stimulation with IL-1. The quantification of this blot is shown on the right. (B) WT MEFs and IκBα^{-/-}β^{-/-}ε^{-/-} cells were stimulated with IL-1 and phosphorylation of p105, p65 and IκBα was analyzed by western blotting. (C) Hyperactivation of NFκB-independent IKKβ-induced autophagy. NEMO-deficient cells stably expressing constitutively active IKKβ and WT or ZF deleted NEMO were stained for LC3 and Hoechst and analyzed by immunofluorescence microscopy. Representative images are shown. Quantification of LC3 positive cells is shown

on the right (% cells with LC3 puncta, mean \pm standard deviation, $n > 150$ cells, $*p < 0.05$). **(D)** Western blot analysis of phosphorylated S6K (T389) and AMPK α (T172) in NEMO-deficient cells stably expressing IKK β EE and indicated NEMO construct. **(E)** NEMO-deficient cells reconstituted with WT or mutant NEMO were starved with HBSS for 1h prior to immunofluorescence staining and analysis. The quantification of LC3 positive cells is shown on the right (% cells with LC3 puncta, mean \pm standard deviation, $n > 150$ cells, $*p < 0.05$). See also Figure S6.